AD_____

Award Number: DAMD17-02-1-0675

TITLE: Preparative Production of Acetylcholinesterase and Paraoxonase in Procaryotic and Eucaryotic Expression Systems

PRINCIPAL INVESTIGATOR: Joel L. Sussman, Ph.D.
I. Silman, Ph.D.

CONTRACTING ORGANIZATION: Weizmann Institute of Science
Rehovot 76100, Israel

REPORT DATE: July 2004

TYPE OF REPORT: Annual

PREPARED FOR: U.S. Army Medical Research and Materiel Command
Fort Detrick, Maryland 21702-5012

REPORT DOCUMENTATION PAGE

Form Approved
OMB No. 074-0188

1. AGENCY USE ONLY (Leave blank)	2. REPORT DATE	3. REPORT TYPE AND DATES COVERED
	July 2004	Annual (1 Jul 2003 - 30 Jun 2004)

4. TITLE AND SUBTITLE
Preparative Production of Acetylcholinesterase and Paraoxonase in Procaryotic and Eucaryotic Expression Systems

5. FUNDING NUMBERS
DAMD17-02-1-0675

6. AUTHOR(S)
Joel L. Sussman, Ph.D.
I. Silman, Ph.D.

7. PERFORMING ORGANIZATION NAME(S) AND ADDRESS(ES)
Weizmann Institute of Science
Rehovot 76100, Israel

E-Mail: Joel.sussman@weizmann.ac.il

8. PERFORMING ORGANIZATION REPORT NUMBER

9. SPONSORING / MONITORING AGENCY NAME(S) AND ADDRESS(ES)
U.S. Army Medical Research and Materiel Command
Fort Detrick, Maryland 21702-5012

10. SPONSORING / MONITORING AGENCY REPORT NUMBER

11. SUPPLEMENTARY NOTES

12a. DISTRIBUTION / AVAILABILITY STATEMENT
Approved for Public Release; Distribution Unlimited

12b. DISTRIBUTION CODE

13. ABSTRACT (Maximum 200 Words)

Members of the serum paraoxonase (PON) family have been identified in mammals and other vertebrates, and in invertebrates. PONs exhibit a wide range of physiologically important hydrolytic activities, including drug metabolism and detoxification of nerve agents. PON1 and PON3 reside on high-density lipoprotein (HDL, 'good cholesterol') and are involved in the prevention of atherosclerosis. We describe the first crystal structure of a PON family member, a variant of PON1 obtained by directed evolution, at a resolution of 2.2 A. PON1 is a six-bladed beta-propeller with a unique active site lid that is also involved in HDL binding. The three-dimensional structure and directed evolution studies permit a detailed description of PON1's active site and catalytic mechanism, which are reminiscent of secreted phospholipase A2, and of the routes by which PON family members diverged toward different substrate and reaction selectivities.

14. SUBJECT TERMS
X-ray crystallography, directed evolution, organophosphates, bioscavangers, enzymatic specificity å

15. NUMBER OF PAGES
34

16. PRICE CODE

17. SECURITY CLASSIFICATION OF REPORT	18. SECURITY CLASSIFICATION OF THIS PAGE	19. SECURITY CLASSIFICATION OF ABSTRACT	20. LIMITATION OF ABSTRACT
Unclassified	Unclassified	Unclassified	Unlimited

Table of Contents

Cover.....1

SF 298.....2

Table of Contents.....3

Introduction.....4

Body.....6

Key Research Accomplishments.....28

Reportable Outcomes.....29

Conclusions.....31

References.....32

Appendices.....34

Introduction

Serum paraoxonase (PON1) is a mammalian enzyme that catalyzes the hydrolysis and, thereby, inactivation of various organophosphates (OPs), including the nerve agents sarin and soman[1]. In recent years it has become apparent that PON1, and its two known Q and R isoenzymes, also play important roles in drug metabolism and in prevention of atherosclerosis[1,2]. PON1 is the best-studied member of a family of mammalian enzymes that includes PON2 and PON3, which share ~60% sequence identity with PON1. PON1 and PON3 reside in the cholesterol-carrying particles HDL ("good cholesterol"), whereas PON2 is found in many tissues. Polymorphism of the PON1 gene affects the blood levels of PON1 and its catalytic efficacy; both factors have a major impact on the susceptibility to atherosclerosis, and to pollutants and insecticides[1]. Mice lacking PON1 are highly susceptible to atherosclerosis and to OP poisoning[3]. *In vitro* assays show that PON1 and PON3 inhibit lipid oxidation in LDL ("bad cholesterol"), thus reducing levels of oxidized lipids involved in the initiation of atherosclerosis[4,5]. Since atherosclerosis is the underlying cause of 50% of mortality in Western societies, and OPs comprise an environmental risk as well as a terrorist threat, PONs have become the subject of intensive research.

Despite many efforts, the structure and mechanism of action of PONs have remained enigmatic. The name, paraoxonase, is purely historical, since the PON family is a hydrolase family with one of the broadest specificities known. PON1 is a proficient esterase towards several synthetic substrates, whilst PON2 and PON3 exhibit high lactonase activity. But the paraoxonase activity of PON1 is rather weak, and PON2 and PON3 exhibit almost no paraoxonase activity[1]. However, all these activities towards man-made chemicals are promiscuous activities of PONs rather then their primary functions. A variety of physiological roles have been proposed for PONs, including phospholipase A2 action[6], degradation of oxidized lipids[7]), and hydrolysis and inactivation of homocysteine thiolactone - a known risk factor for atherosclerotic vascular disease[8]. The anti-atherosclerotic activity of the PONs is intimately linked to their localization on HDL particles. It has been suggested that the hydrophobic N-terminus of PON1 mediates its anchoring to HDL[9].

Structural and functional characterization of the PONs, and their engineering, have been hindered by lack of an ample source of recombinant protein. We recently described the directed evolution of PON1 and PON3 variants that express in a soluble and active form in *E. coli*, and

exhibit enzymatic properties identical to those reported for PONs purified from sera[10]. We report the crystal structure of a recombinant PON1 variant derived from rabbit PON1, which is highly similar to human PON1. By combining directed evolution, site-directed mutagenesis and kinetic studies, we provide a comprehensive description of the overall architecture of PON1, details of its active site, catalytic mechanism and HDL-binding mode. We show how directed evolution in the laboratory follows the footsteps of natural evolution in swiftly providing new PON variants with pre-determined catalytic specializations.

Body

Crystallization and structure determination

Previous attempts to determine the structure of PON1 relied on limited amounts of serum-purified proteins, resulting in crystallization of a protein that co-purified with it[11]. Human PON1 is rather unstable, and tends to aggregate in the absence of detergents[12]. These factors led us to directly evolve PONs for bacterial expression and increased solubility[10]. Family shuffling of four PON1 genes (human, rabbit, mouse and rat), and screening for esterolytic activity, led to recombinant PON1 variants (rePON1s) that express in *E. coli*. These variants diverged from wild-type (wt) rabbit PON1 by 14-31 amino acids coming from other PON1 genes, and exhibit enzymatic properties essentially identical to those of wt PON1[10]. Variants from the 1st round of evolution aggregated, and none crystallized. The 2nd-generation variants (obtained by shuffling of the 1st generation variants and screening for highest expression levels) did not aggregate, and at least one (G2E6) gave stable and well diffracting crystals.

RePON1-G2E6 exhibits 91% identity to wt rabbit PON1, with the vast majority of variations deriving from human, mouse, or rat wt PON1. It should be noted that rabbit and human PON1s are also highly homologous in sequence (86%) and function[13]. Moreover, sequence variations between rePON1-G2E6 and rabbit and human PON1 are in regions that do not affect their active sites or overall structures. Both purified native rePON1-G2E6 and rePON1-G2E6 containing selenomethionine (SeMet- rePON1-G2E6) were crystallized, yielding isomorphous crystals of space group $P4_32_12$. The structure was solved by single isomorphous replacement anomalous scattering from data collected to 2.6Å on the SeMet crystals and to 2.2 Å on the crystals of the native protein[14]. The structure shows all residues except N-terminal residues 1-15 and a surface loop (72-79). Two calcium atoms, a phosphate ion, and 115 water molecules are also seen.

The overall architecture of PON1

PON1 is a 6-bladed β-propeller, with each blade containing 4 strands (Fig. 1). The 'velcro' closure characteristic of this fold[15] is supplemented by a disulphide bridge between Cys42 (strand 6D) and Cys353 (strand 6C). This covalent closure of the N- and C-termini is rarely seen in β-propellers with more than four blades, but is conserved throughout the PON family.

Two calcium ions, 7.4Å apart, are seen in the central tunnel of the propeller: one at the top (Ca-1) and one in the central section (Ca-2). Ca-2 is most probably a 'structural calcium' whose dissociation leads to irreversible denaturation[16]. Ca-1 is assigned as the 'catalytic calcium'[16]. It appears to interact with five protein residues (the side-chain oxygens of Asn224, Asn270, Asn168, Asp269 and Glu53), 2.2-2.5Å away. Two other potential ligands are a water molecule, and one of the oxygens of a phosphate ion. The two calcium ions exhibit markedly different affinities[13]. The ligation of Ca-1 is more extensive than that of Ca-2's. However, two of Ca-1's ligating residues (Asn224, Asp269) exhibit distorted dihedral angles. This, and the higher solvent accessibility of Ca-1, indicate that Ca-2 is the higher affinity calcium.

PON1's structure resembles that of *Loligo Vulgaris* DFPase[17]. Both are 6-bladed propellers with two calcium atoms in their central tunnel. They also share functional homology, since both exhibit phosphotriesterase (PTE) activity, although PON1 is primarily an esterase or lactonase. However, there is no clear sequence homology between them (BLAST E-score >>3.6), although more sensitive algorithms indicate weak but significant similarity[11]. Closer inspection reveals that PON1 and DFPase differ significantly in their overall architecture, active-site structure and mechanism. In particular, PON1 possesses a unique addition in the form of an active-site canopy defined by helices H2 and H3 and the loops connecting them to the β-propeller scaffold. This addition provides PON with an uncharacteristically closed active site, since most β-propellers, including DFPase, exhibit uncovered active sites defined only by loops that connect the β-strands. It seems to play a critical role in PON1's function, both in defining the active-site architecture and sequestering it from solvent, and in anchoring PON1 to HDL.

Although detergent-solubilized PON1 forms dimers and higher oligomers[12], in the crystal there is only one molecule per asymmetric unit, and very few contacts between symmetry-related molecules. It is possible that crystallization favors a monomeric form, but it seems more likely that oligomerization of PON1 is a consequence of its anchoring to detergent micelles in a mode similar to its anchoring to HDL. Mammalian PON1 is glycosylated, but glycosylation is not essential for hydrolytic activity[10,18]. There are four potential *N*-glycosylation sites on PON1 (NX(S/T) sites). Two, Asn227 and Asn270, are in the central tunnel of the propeller, and are

largely inaccessible to solvent. Asn253 and Asn324 are located on surface loops, and are most probably, as previously proposed[18], PON1's glycosylation sites.

Directed evolution of substrate specificity

Site-directed mutagenesis is routinely used to identify active-site residues. This approach suffers, however, from a well-recognized drawback: Loss of activity does not necessarily indicate direct involvement of a particular amino acid in the protein's function since mutations often disrupt the overall structure. Indeed, whereas certain residues identified by site-directed mutagenesis as being essential for PON1's activity[18-20] are related to its active site, others are not (e.g., Trp281). In contrast, mutations identified following directed evolution towards a modified function are inevitably relevant to activity, and involve residues located within, or in the vicinity of, the active site.

Gene-libraries of rePON1 were prepared by random mutagenesis and cloned in bacterial colonies as described[10]. Colonies on agar plates were screened with several different substrates representing each of the substrate-reaction types catalyzed by PONs: PTE, lactonase and esterase. For the latter, both acetate and octanoate esters were employed, representing, respectively, 'short chain' esters towards which PON1 exhibits high activity, and 'long chain' esters, that are typical substrates of lipases for which PONs exhibit lower activity. The best clones identified from a screen of 10^3-10^4 library clones were shuffled, and the resulting libraries screened for the same activity. Two to four rounds of selection were performed, after which the sequences and catalytic activities of the selected variants were determined (Table 1).

The newly evolved variants clearly define a set of amino acids the alteration of which dramatically shifts PON1's reactivity and substrate selectivity (Table 1). These shifts involve not only an increase of 16-46-fold in activity towards the substrate for which each particular variant was evolved, but also a drastic decrease in activity on substrates which had not been selected for (6-167-fold). Overall, shifts in substrate selectivity of up to 4,600-fold were observed. Thus, for example, variant 7HY exhibits relative to wt PON1, 46-fold higher long-chain esterase activity and 100-fold lower PTE activity. Some of the new variants, all derived from PON1, represent substrate and reaction selectivities more similar to PON2 or PON3. For example, variants 2AC

and 1HT exhibit ~20-fold higher esterase and lactonase activity relative to PON1, and 5-30-fold weaker PTE activity. The positions identified by directed evolution all appear in the same region at the top of the β-propeller. They clearly delineate the entrance to and walls of PON1's active site (Fig. 2).

The catalytic mechanism

At the very bottom of the active-site cavity lie both the upper calcium (Ca-1) and a phosphate ion, which was present in the mother liquor (Fig. 2b). One of the oxygens of this phosphate is only 2.2Å from Ca-1, and it may be bound in a mode similar to the intermediates in the hydrolytic reactions catalyzed by PON. One of its negatively charged oxygens that nearest to Ca-1, may mimic the oxyanionic moiety of these intermediates stabilized by the positively-charged calcium. This type of 'oxyanion hole' is seen in secreted phospholipase A2 (PLA2)[21], and has also been suggested for DFPase[17]. Two other phosphate oxygens may be mimicking the attacking hydroxyl ion and the oxygen of the alkoxy or phenoxy leaving groups of ester and lactone substrates.

To help elucidate the mechanism of action of PON we determined its pH-rate profile with two typical substrates: an ester, 2-naphthyl acetate (2NA), and a phosphotriester, paraoxon. Both profiles exhibit a bell-shaped curve. The minor basic shoulder fits an apparent pK_a of 9.8 (paraoxon) or 9.0 (2NA), probably reflecting the deprotonation of a basic side-chain that affects the active site but is not directly involved in catalysis. The fully pronounced acidic shoulder, of apparent pK_a ~7.1, may be ascribed to a His imidazole involved in a base-catalyzed, rate-determining step. In hydrolytic enzymes, His often serves as a base, deprotonating a water molecule and generating the attacking hydroxide ion that produces hydrolysis. In secreted PLA2, the attacking hydroxide is generated by a His-Asp dyad, in which the imidazole acts as a base to deprotonate a water molecule, and the Asp carboxylate increases the imidazole's basicity via a proton-shuttle mechanism. The closest His nitrogen in PLA2 is 6.3Å from the catalytic calcium, and two water molecules are involved: one attacking the substrate (after deprotonation), and another 'catalytic water' that mediates between the attacking water and the His base[21]. The DFPase active site also contains a His-Glu dyad with a His nitrogen 7.2Å from the catalytic calcium[17].

Did PON1 adopt the same mechanism – namely a His-Glu/Asp dyad acting as base on a two-water-molecule cascade? PON1's active site contains such a dyad (Asp183, His184). However, His184 is ~11Å from Ca-1, and the His184Asn mutant of human PON1 is active[20]. Another putative dyad is His285-Asp269. Yet Asp269 ligates Ca-1, and His285 is ~8Å from Ca-1 and ~5Å from the nearest phosphate oxygen. We identified, however, a His-His dyad near both Ca-1 and the phosphate ion (Fig. 3). We hypothesized that His115 (the closer nitrogen of which is only 4.1Å from Ca-1) acts as a general base to deprotonate a *single* water molecule and generate the attacking hydroxide, while His134 acts in a proton shuttle mechanism to increase His115's basicity. Interestingly, His115 adopts distorted dihedral angles - a phenomenon observed in catalytic residues of many enzymes. This assignment for the catalytic mechanism was supported by the His115Gln mutation, which resulted in a dramatic decrease (~$2x10^4$ fold) in activity, and the His134Gln, that produced a smaller, but substantial, decrease (6-150 fold).

However, following a recent report by Yeung and coworkers[22]who introduced the His115Trp mutation into human PON1, that is highly homologous to our recombinant PON1, we carried out further mechanistic studies. We thus discovered that our previous measurements of the His115Gln and His134Gln mutants were biased by two factors. First, the His115Gln mutant accidentally carried another mutation (His177Arg) incorporated during by PCR amplifications of the gene. We found that, in itself, this mutation in a residue far way from the active-site, has little effect (paraoxonase and aryl-esterase activities are 70% of that of the parental PON1 gene). But the double His115Gln/His177Arg mutation led to an almost complete loss of activity as reported in the original article. Second, both mutants (His115Gln and His134Gln) are unstable and prone to loss of activity, misfolding, and ultimately aggregation. We have now regenerated the same mutants (including the His115Gln in isolation), purified them with the permanent presence of detergent (0.1% tergitol; in the lysis, loading and elution buffers) and 10% glycerol, and assayed them immediately after. Their activities are display in Table 2.

The existence (or even increase) in the paraoxonase activity of these mutants suggests that the new purification conditions, and the removal of the accidental His177Arg mutation excluded the global effect of these mutations on the protein stability and folding. Furthermore, we have

since incorporated the same mutations into the recombinant PON1 variant G2E6, the one whose 3D structure was determined[14,23] and into another recombinant PON1 variant, G3C9, with similar results. Thus our most recent data suggest that His115 and His134 are not responsible for the paraoxonase activity of PON1, although they appear to significantly affect its aryl-esterase activity. Thus, the possibility must be considered that the two hydrolytic activities are catalyzed by different active-site residues, and that the His-dyad model postulated (Fig. 3) may be valid only for the aryl-esterase activity.

Cys284, which is conserved in all PONs, has been proposed to fulfill alternative functions of PON1 related to atherosclerosis[24]. It is part of a highly conserved stretch that includes active-site His285, and is packed against four highly-conserved residues from the adjacent strands (267, 268, 303 and 305; Fig. 4). Since it is buried, it is unlikely that it has a functional role. Its mutation, however, is likely to destabilize the core structure, thereby affecting function indirectly. Indeed, we found that Cys284 mutants of rePON1 are poorly expressed and relatively unstable.

Anchoring of PON1 to HDL

PON1 and PON3 are synthesized in the liver, and secreted into the blood, where they specifically associate with HDL. HDL is a particle of ~10 nm diameter, composed primarily of membrane components (phospholipids, cholesterol and cholesterol esters), and apolipoprotein A-I (apoA-I)[25], the amphipathic helices of which are thought to wrap around the particle's membrane-like bilayer in a belt-wise manner[26].

PON1 retains its hydrophobic N-terminus, which resembles a signal peptide, and is thought to be involved in anchoring of PON1 to HDL[9]. Most of the N-terminus is disordered and invisible in the crystal structure;, yet its hydrophilic part, which extends beyond the signal peptide (residues 19-28), adopts a helical structure (H1). The entire sequence of the N-terminus is compatible with a transmembrane helix, yet following a secondary structure prediction, we modeled only residues 7-18 as part of H1 (Fig. 5). Helix H2, adjacent to H1, possesses a clearly amphipathic character. Unexpectedly, however, its hydrophobic face points towards the solvent, as do several residues from the two loops that connect H2 to the propeller scaffold. Helices H1

and H2 form, therefore, two adjacent hydrophobic patches that clearly provide a potential membrane-binding surface (Fig. 5a). The interface with HDL was further defined by a characteristic 'aromatic belt' rich in Trp and Tyr side chains, and a Lys side chain on H1[27]. Notably, the glycosylation sites point away from the interface (Fig. 5b).

The crystal structure reveals the overall fold of the PON family, and the details of the 3D structure of PON1, and permits the presentation of a plausible catalytic mechanism. Such a mechanism, based on a His-dyad, has not been described before, although its key elements are reminiscent of secreted PLA2. Catalysis of both C-O and P-O hydrolysis at one site is unusual but not unprecedented[28,29]. The structure, the directed evolution results, the pH-rate profiles, and previous biochemical data[1,10] show that both these activities indeed take place at the same site. There is, however, a possibility that certain PON1 activities (e.g., as a homocysteine thiolactonase[8]) make use of a different subset of residues of this site, including His285, whose side chain also points towards the center of the cavity and to the phosphate ion. In addition, nucleophilic catalysis by His115 cannot yet be ruled out, although there is currently no evidence to support catalysis via an acyl- or phosphoryl-enzyme intermediate.

The 3D-structure does provide a hint regarding the origins of PON1's remarkably wide substrate range. Hydrophobicity is common to almost all its effective substrates. The hydrophobicity and depth of PON1's active site explain this preference, and account for the fact that PON1's substrates, whether poor or effective, exhibit K_M values in the millimolar range, but dramatically different k_{cat} values[1,10]. PON1's multi-specificity is, therefore, driven primarily by non-specific hydrophobic forces, as observed for other enzymes that possess deep hydrophobic active sites, such as acetylcholinesterase[30]. We postulate that poor substrates, as well as effective ones, bind at the active site with similar affinity; yet the mode of binding differs, since the poor substrates are inadequately positioned relative to Ca-1 and to the catalytic base. It seems likely that the mutations observed following the directed evolution process reshape the active site walls and perimeter, thereby improving the positioning of some substrates (and of their respective catalytic intermediates and transition states) and worsening that of others. Reshaping of the active site walls is also the driving force behind the evolutionary divergence of various PON sub-families.

Polymorphism of the PON gene, and its effects on susceptibility to OP poisoning and to atherosclerosis, are the subject of intensive research. The two most common PON1 forms are Q/R192 and L/M55. The 3D structure of the recombinant PON crystallized reveals that Lys192 is part of the active-site wall. In human PON1, this position is normally arginine (R), but a commonly observed polymorphism to glutamine (192Q) results in an approximately 10-fold decrease in paraoxonase activity accompanied by a higher susceptibility to atherosclerosis[1]. Given the drastic effects of changes in other active-site residues on substrate selectivity (Table 3), the human 192Q variant may indeed exhibit significantly reduced activities towards PON1's physiological substrates, resulting in increased susceptibility to atherosclerosis. The Leu55Met mutation may significantly affect PON1's stability, and thereby result in the lower enzymatic activity observed[31]. This may be ascribed to the key role of Leu55 in packing the propeller's central tunnel, and/or to the fact that its neighboring residues (Glu53 and Asp54) ligate both Ca-1 and Ca-2.

Methods

A detailed analysis of the amino acid variations between rePON1 variant G2E6 and wild-type Rabbit PON1

As mentioned above [10], all rePON1 variants that efficiently express in *E. coli* are chimeras of four mammalian PON1s (Human, Mouse, Rat and Rabbit) that show 79- 95% sequence identity by Clustal W analysis (Fig. 6). These PON1 genes were recombined to create the shuffled DNA library. The rePON1 variants were explicitly selected so that their enzymatic properties remain unchanged relative to wild type (wt) PON1. This functional identity was confirmed with over a dozen different substrates, including esters, phosphotriesters, lactones, thiolactones[1], as well as esters of long-chain carboxylic acids. Their biological activities are also very similar to those of wt human and rabbit PON1. Selected variants were found to be most similar to RabPON1 (rabbit PON1) with fewer contributions from the other three parental wild type (wt) genes. Variant G2E6 for which the structure was solved exhibits 91% similarity to RabPON1. Overall, there are 31 amino acid differences between rePON1-G2E6 and wt RabPON1. Twenty eight of these differences come from other wt PON1 genes, and only three are mutations in the real sense. As analyzed below, these differences are all in regions that do not seem to affect the overall structure of the enzyme or its active site.

The amino acid differences between rePON1-G2E6 and wt RabPON1 can be divided to three groups (Table 4). The first group is comprised of 8 residues that originate from the other parental genes (Human, Mouse and Rat) and were found to be mostly within the interior of the protein (Fig. 7). These residues are conserved among all rePON1 variants that efficiently express in *E. coli* ([10] and Fig. 6). The structure indicates that several of these residues are in contact with each other. For example, Leu130 and Val143 that pack strand 2B against 2C, or Val320 (strand 5D), and Leu341 and Ile343 (strand 6B), that are critically located at the propeller's hydrophobic core between the fifth and the sixth blades. Residues of the first group most probably facilitate better packing of the hydrophobic core, and prevent misfolding and aggregation. Their absolute conservation amongst the rePON1 variants indicates that they are the key to soluble expression in *E. coli*. Their location, distant from the active site, explains why all the rePON1 variants exhibit enzymatic activity similar to that of wt PON1. The second group includes amino acid that are not conserved among other rePON1 variants (e.g. rePON1-G3C9), yet originate from the other parental PON1 genes (Human, Mouse and Rat). These amino acids are located mostly on the protein surface (Fig. 7). Three of these residues (105, 107, 297) are involved in intermolecular contacts in the crystal. Hence they probably facilitate the successful crystallization of rePON1-G2E6. Most of the residues are far from the active site, at the bottom

face of the propeller. Only one residue, Phe293, is part of PON1's active site. However, this residue anyway varies between Tyr (e.g., RabPON1) or Phe (e.g., Human PON1, Mouse PON1 and Rat PON1; Fig. 6) in various wt PON1s that are known to exhibit almost identical enzymatic properties.

The third, and smallest, group includes three residues that were mutated during the shuffling and amplification processes and differ, therefore, from all four parental genes. These residues are all located on the protein surface (Fig. 7), and include positions 19, 123 and 260. Position 19 (Gly to Arg) varies between the different wt PON1s (Fig. 6) that are known to exhibit almost identical enzymatic properties. In addition this position was mutated during the directed evolution of PON1 and selected (data not shown) without having any observable effect on the enzymatic activity. The mutation at position 123 (Glu to Asp) is subtle; this residue is located on the surface and, therefore, is highly unlikely to have any effect on the enzymatic function. The third residue (260) was mutated from Lys to Arg. This is also a subtle mutation that, being on the surface, is unlikely to change the protein's properties.

In conclusion, it seems that none of the sequence variations seen between rePON1- G2E6 and wt rabbit PON1 are likely to affect its structure or function. PON1 appears to be insensitive to mutations at many positions, and can tolerate multiple amino acid substitutions at its surface and core, with no effect on its enzymatic function.

Expression and purification of native rePON1-G2E6 and its SeMet derivative

rePON1-G2E6 was expressed as a thioredoxin (Trx) fusion protein, with an incorporated HIS Tag, and purified by chromatography on a NiNTA column followed by High Trap Q column (Pharmacia) [10]. During attempts to purify and crystallize it, we noticed that during storage the linker between the Trx and rePON1 was spontaneously cleaved, and the crystals were comprised only of rePON1. The origins of this cleavage are still under investigation. It was observed in all rePON1 variants, and could even be mediated by PON1 itself. Subsequent crystallizations were set up with the cleaved and purified rePON1 as described below. Following purification of the Trx fusion product by Ni-NTA and ion exchange chromatography[10], the protein was incubated at 25°C for ten days. The cleavage was monitored by SDS-PAGE and mass spectrometry. The cleaved protein was concentrated and applied to HiLoad 26/60/ Superdex 200 (preparative grade, Pharmacia). Fractions from the main peak were analyzed again by SDS-PAGE, and enzymatic activity, pooled, and concentrated to 10mg/ml. Sodium azide was added to a concentration of

0.02%. Mass spectrometry indicated a mass of 40223±201Da. N-terminal Edman sequencing gave the following a sequence: H2NDDDKAM. Both types of data are consistent with cleavage of the linker (expected mass spec 40108Da) 5 amino acids before the methionine residue that is PON1's first amino acid.

The SeMet-labeled rePON1-G2E6 was obtained as follows: a pET 32b plasmid containing rePON1-G2E6[10] was freshly transformed into B834(DE3) cells and plated on LB agar plates supplemented with Ampicillin. Colonies from three agar plates were scraped and rinsed (by resuspension and centrifugation) with M9 salt solution supplemented with 2mM $MgSO_4$, 0.4% Glucose, 25 μg/ml $FeSO_4$, 40 μg/ml of each of the 20 natural amino acid except L-methionine, 40μg/ml of seleno-L-methionine, 1μg/ml of vitamins (Riboflavin, Niacinamide, Pyridoxine monohydrochloride and Thiamine) and 100μg/ml of Ampicillin. Typically, 1 L of M9 minimal media with the above supplements was inoculated with 5ml of rinsed *E. coli* colonies and grown at 30°C to OD_{600nm} = 0.7. Cultures were then transferred to 20°C and IPTG added to 0.5mM. Growth was continued for another 36 hours at 20°C, after which the cells were harvested, lysed and purified as above. Mass spectrometry indicated the incorporation of six SeMets per rePON1 including the Trx tag. Purification, cleavage from Trx and isolation of rePON1 were performed as above.

Structure determination The structure was determined for rePON1 variant G2E6 (for its sequence see Fig. 4). The rePON1 variants were crystallized by the microbatch method under oil[32] using a Douglas Instruments robot IMPAX 1-5 Data were collected on beamline ID14-4 at the European Synchrotron Radiation Facility and processed with XDS[33]. Three datasets were collected for the SeMet protein at 100K at Se peak wavelength (0.9794Å) in order to increase the redundancy and accuracy of the Se anomalous signal while monitoring the extent of radiating damage. A data set of the native crystal was collected at a wavelength of 0.9796Å. Data were collected on beamline ID14-4 at the European Synchrotron Radiation Facility (ESRF) and processed with XDS[33]. Data collection statistics are given in Table 5.

Although PON1 bears no sequence similarity to any other protein sequence, it was suggested that it might have a 6-beta propeller conformation. As a consequence, we attempted to solve its

structure by molecular replacement (MR) using the structure of 3-carboxy-cis, cis-muconate lactonizing enzyme (PDB-code 1jof) as a search template. A weak, but still significant, MR peak was found by the maximum likelihood program PHASER[34]. Although this did not result in structure solution, it did help in selecting the correct space group ($P4_32_12$). Three Se sites were located on the basis of the anomalous difference, using SHELXD after local scaling using XPREP[35]. SHELXE confirmed the correct space group and solvent content. Good experimental SIRAS (single isomorphous replacement anomalous scattering) phases were obtained using the program SHARP[36] while refining 3 Se sites against the 2.2Å native and 2.6Å Se SAD data, resulting in an overall figure of merit (FOM) of 0.11/0.06 for the acentric/centric reflections respectively. The isomorphous difference phasing power was very low (0.22 overall) due to the lack of isomorphism between the native and SeMet data sets. However, the anomalous phasing power for the SeMet SAD data set was good to at least 4Å (0.74 overall). Phases were improved by applying solvent flipping density modification using SOLOMON[37], as directed by SHARP using a 63% solvent content, giving an overall FOM of 0.88. An automated tracing program ARP/wARP[38], using native amplitudes to 2.2Å, coupled with experimental phase restraints, resulted in an automatic tracing of ca. 95% of the chain. Manual model completion was performed using program O[39], iterated with refinement using REFMAC[40]. The refinement and model statistics are listed in Table 5.

Figures were created with PyMol (http://pymol.sourceforge.net/) and MolScript (Fig. 3; http://www.avatar.se/molscript). Accessible surface area was calculated by the program AREAIMOL in the CCP4 package[41]. Coordinates were deposited in the PDB, entry 1v04.

Directed evolution rePON1 variant G3C9 was used as the starting point for directed evolution. It exhibits a sequence almost identical to those of wt rabbit PON1 and rePON1 variant G2E6, whose 3D-structure was determined (91% identity), and the same enzymatic parameters. Libraries were generated and cloned as described[10]. PTE activity was screened, and subsequently quantified, with the fluorogenic OP substrate, 7-*O*-diethylphosphoryl-3-cyano-7-hydroxycoumarin as described[10]. Thiolactonase activity was initially screened for with 2NA on agar plates. Positive clones were picked from replica plates and grown in 96-well plates as described[10]. The crude cell lysates and purified proteins were assayed for hydrolysis of γ-

butyrothiolactone using 5,5'-dithio-bis-2-nitrobenzoic acid for detection of product by absorbance at 412 nm. Esterase activity was screened with the fluorogenic substrate 7-acetoxycoumarin (for short-chain esterase activity), or with 2-naphthyl octanoate (for long-chain esterase activity) using fast red for the detection of 2-naphthol[10]. Colonies exhibiting the highest activity were grown in 96-well plates, and the crude cell lysate was assayed spectrophotometrically at 365 nm, for hydrolysis of 7-acetoxycoumarin, and at 320 nm with 2-naphthyl laurate. The activity of the variants described above was determined with the same substrates and assays.

Enzyme kinetics k_{cat} and K_M values were determined for rePON1-G2E6 with 2NA and paraoxon[10], at pH 5.69.5. Buffers used were MES (pH 5.6–6.5) and bis-tris propane (pH 6.5–9.4) at 0.1M, plus 1mM $CaCl_2$; the ionic strength was adjusted to 0.2M with NaCl. Kinetic parameters were obtained from 3–5 independent measurements averaged with standard deviations of 2–23%.

Tables

Table 1. New PON1 variants generated by directed evolution

Variant		Phospho-triesterase activity[a]	Lactonase activity[a]	Esterase activity[a]	
				short chain **ester**	***long chain*** **esters**
rePON1 (wt-like activity)		$3.5*10^3$	$1.4*10^2$	$3.0*10^4$	$1.7*10^2$
DIRECTLY-EVOLVED VARIANTS WITH 'SPECIALIZED' SUBSTRATE SELECTIVITIES					
#	**Mutations**[b]				
7PC	**V346A**	$1.3*10^4$ **(3.7)**[b]	$5.0*10^1$ (0.36)	$1.4*10^3$ (0.05)	$1.4*10^1$ (0.08)
4PC	**L69V, S193P, V346A**	$5.7*10^4$ **(16.3)**	0.9 (0.006)	$4.4*10^2$ (0.015)	n.d
1HT	**I291L, T332A,** G339E	$6.0*10^2$ (0.17)	$3.0*10^3$ **(25.9)**	$8.6*10^3$ (0.3)	n.d.
2AC	**F292S, V346M** V30A, E249K	$1.1*10^2$ (0.03)	6.4 (0.04)	$6.0*10^5$ **(20)**	$7.0*10^2$ (4.1)
7HY	**F292V, Y293D,** I109M	$4.1*10^1$ (0.01)	4.1 (0.03)	$1.2*10^5$ (4.0)	$8.0*10^3$ **(47)**
4HY	**I74L, F292L** K84Q, I343M	$5.3*10^1$ (0.015)	5.9 (0.04)	$5.2*10^4$ (1.7)	$6.5*10^3$ **(38)**

[a]Activities are expressed as μmoles of product released per minute per mg enzyme. In parentheses are the activities of the new variants relative to wt PON1's activity on the same substrate.

[b] Mutations are given in relation to the sequence of the wt-like variant G3C9. In bold are positions found to be mutated in all the highest-activity variants for a given substrate. Typically, the same mutations could be individually identified in the sequence of selected variants from the 1st and 2nd rounds of evolution, and appear together in the 3rd generation variants. Mutations that appear in only one selected variant, but not in others selected for the same substrate, and/or do not appear in the 1st and 2nd round of evolution, are noted in regular print.

Table 2 New PON1 variants generated by site-directed mutagenesis

Mutation	Aryl-esterase (% relative to wt)	Paraoxonase (% relative to wt)
His115Gln	0.6%	32%
His115Trp	0.056%	195%
His134Gln	9.9%	600%

Table 3. Selectivity-determining residues of PONs

Sub-family	PON1	PON2	PON3	Newly-evolved PON1s	
Position				Residue	Selectivity
69	L	L	L	V/I	PTE[a]
74[b]	I	L	M	L/M	lactonase/esterase
75[b]	K/M	K/H	P		
76[b]	S	S	N/A		
78[b]	N/D	A	A		
190	Y	F/I	L/V/F		
192	K/R	K/M	S/A/V		human R/Q SNP
193	S	Y/F	F/L	P	PTE[a]
196	M	M/T	M		
222	F	S	S		
240	L	I	V		
291	I	L/V	L	L	Lactonase
292	F	F/Y	L	L/V/S	Esterase
293	F/Y	V/Y/I	N/I	D	lipase-like[c]
332	T	S	S/T	A	Lactonase
346	V	L/V	I/V	A	PTE[a]

[a] PTE = phosphotriesterase. It should be noted that the PTE activity of these mutants is much higher than that of wt PON1 which is the best PTE of the three PONs (Table 1).

[b] Residues 74–79 belong to the selectivity-determining residues which differ between the PON subfamilies (Fig. 4) but are conserved within them. These residues are part of a mobile loop (72–79) containing residue 74, which is not seen in the electron density but is presumably part of the active site.

[c] Lipase-like activity refers to esters of long-chain carboxylic acids (Table 1).

Table 4. Amino acid changes in G2E6 relative to Rabbit PON1

Group	Mutations[a]	Origin	Location and nature[c]
I	T126, L130, S138, V143, G301, V320, L341, I343	wild type Human, Mouse, Rat, PON1	hydrophobic core; conserved residues among all soluble PON variants.
II	M12, K93, E94, A96, S98, E101, I103, N105, L107, I109, I121, E149, V261, S263, D265, F293, A296, E297, E313, D354.	wild type Human, Mouse, Rat, PON1	protein surface; non-conserved between different soluble PON1 variants.
III	R19, D123,R260	Mutation[b]	protein surface

[a] The rePON1-G2E6 sequence was aligned to the rabbit PON1 protein sequence using ClustaWI. Amino acid identities are to the rePON1-G2E6 sequence.

[b] Mutations that occurred during the shuffling process into an amino acid that is different relative to all four wt PON1 genes.

[c] The precise locations of these amino acids on PON1's structure are shown in Fig. 7.

Table 5 Data collection and refinement statistics.

Data collection

	Native	SeMet protein
Wavelength (Å)	0.9796	0.9794
Unit cell (Å)	98.44, 139.17	98.49, 139.56
Space group	$P4_32_12$	$P4_32_12$
Resolution range (Å)	20–2.2	30–2.6
Number of unique reflections	35,312	39,473
Completeness (%)[a]	99.7 (97.9)	97.8 (97.7)
$I/\sigma(I)$[a]	12.7 (2.7)	13.7 (4.2)
$R_{sym}(I)$ (%)[a]	8.6 (66.1)	10.4 (51.0)

Refinement and model statistics

Resolution range (Å)	20–2.2
Number of reflections	33,505
R-factor: work, free (%)	18.5, 21.7
Average B-factors ($Å^2$)	34.76
RMSD from ideal values:	
Bond length (Å)	0.028
Bond angle (°)	2.02
Dihedral angles (°)	28.7
Improper torsion angles (°)	2.06
Estimated coordinate error:	
Low resolution cutoff (Å)	5.0
ESD from Luzzati plot (Å)	0.32
ESD from SIGMAA (Å)	0.34
Ramachandran outliers (%)[b]	3.9

[a] Data for the outer shell given in parentheses.

[b] Ramachandran plot outliers are all glycines except for H115, N224, D269 and H348.

Figures

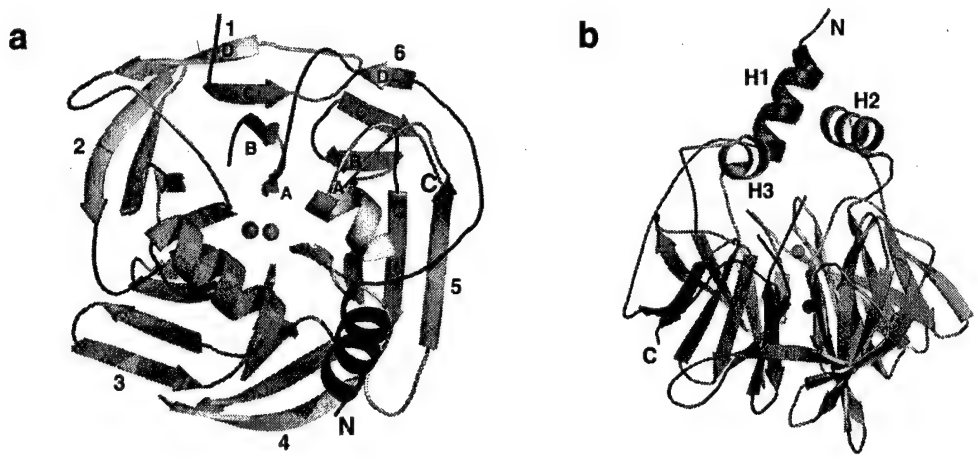

Fig. 1. Overall structure of PON1. (**a**) A view of the 6-bladed β-propeller from its top. The top of the propeller is, by convention, the face carrying the loops connecting the outer β-strand of each blade (strand D) with the inner strand (A) of the next blade[17]. Shown are the N- and C-termini, and the two calcium atoms in the central tunnel of the propeller (Ca-1 in green, Ca-2 in red). (**b**) A side view of the propeller, including the three helices at the top of the propeller (H1–H3). N-terminal residues 1–15, and a surface loop connecting strands 1B and 1C (residues 72–79) are not seen in the structure.

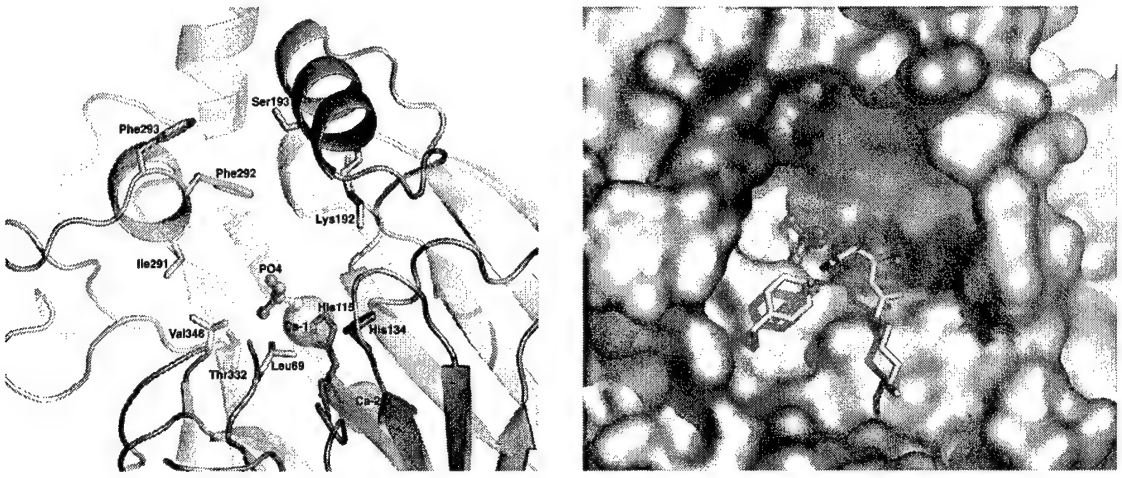

Fig. 2. The active site of PON1 viewed from above the propeller. (**a**) Shown are the central tunnel of the propeller with the two calcium atoms, and the side-chains of the residues found to be mutated in the newly-evolved PON1 variants for esterase and lactonase (in orange) or for PTE activity (in yellow), including position 192 of the Q/R (Gln/Arg) human polymorphism. Shown in red is the putative catalytic His-dyad (see *The catalytic mechanism* section and **Fig. 3**). (**b**) A surface view of the active site. Lys70, Tyr71and Phe347 are shown as sticks to permit a better view of the active site. At the deepest point of the cavity lies the upper calcium atom (Ca-1 in green) to which a phosphate ion (PO4) is bound.

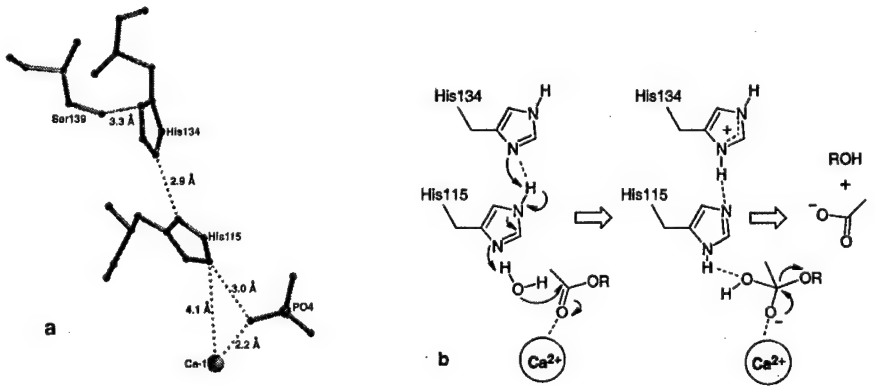

Fig 3. The postulated catalytic site and mechanism of PON1. (**a**) The catalytic site: the upper calcium atom (Ca-1), the phosphate ion found at the bottom of the active site, and the postulated His-dyad. (**b**) A schematic representation of the proposed mechanism of action of PON1 on ester substrates such as phenyl and 2-naphthylacetate. The first step involves deprotonation of a water molecule by the His-dyad to generate an hydroxide anion which attacks the ester carbonyl, producing an oxyanionic, tetrahedral intermediate. This intermediate breaks down (second step) to an acetate ion and either phenol or 2-naphthol.

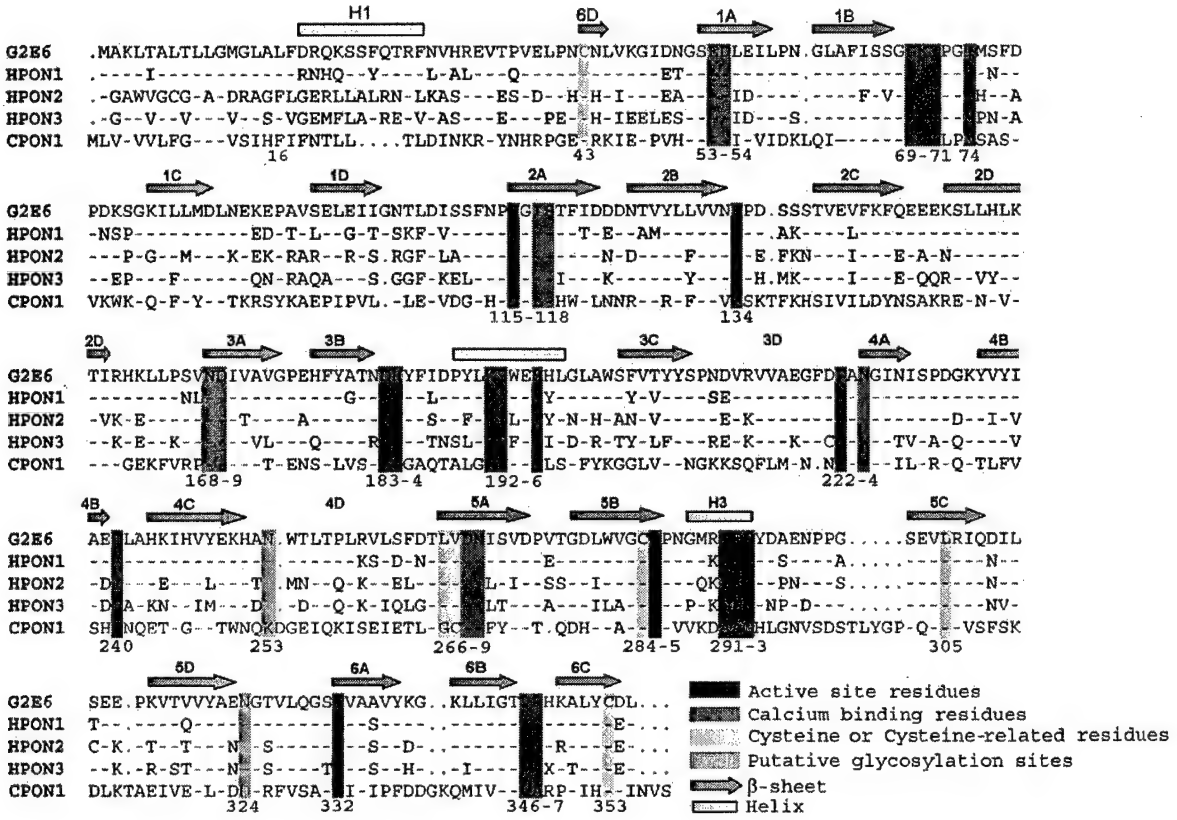

Fig 4. Sequence alignment of representative members of the PON family. Shown are human PON1, PON2 and PON3 (with an 'H' prefix), *C. elegans* PON1 (CPON1), and rePON1 variant G2E6, the structure of which is reported here.

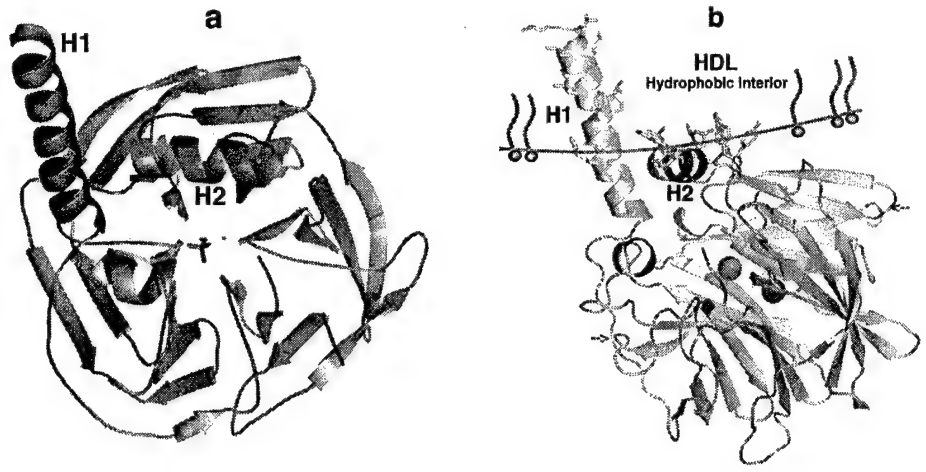

Fig 5. The proposed model for anchoring of PON1 to the surface of HDL. (**a**) Tertiary structure cartoon of rePON1 showing its exposed hydrophobic surfaces. N-terminal residues 7–18, missing in the crystal structure, and predicted to be helical, were modeled as part of H1. Denoted are *all* the hydrophobic residues (L,F,P,I,Y,W,V) appearing with accessible surface area ≥20Å^2. (**b**) Hydrophobic residues proposed to be involved in HDL-anchoring are shown with their side-chains in yellow. The line - defined by the side chains of Tyr185, Phe 186, Tyr190, Trp194, Trp202 (helix H2 and the adjacent loops) and Lys21 (helix H1) - models the putative interface between HDL's hydrophobic interior and the exterior aqueous phase. The active site and the selectivity-determining residues (Table 2) are marked in blue, and the proposed glycosylation sites (Asn253 and Asn324) in red.[13,18]

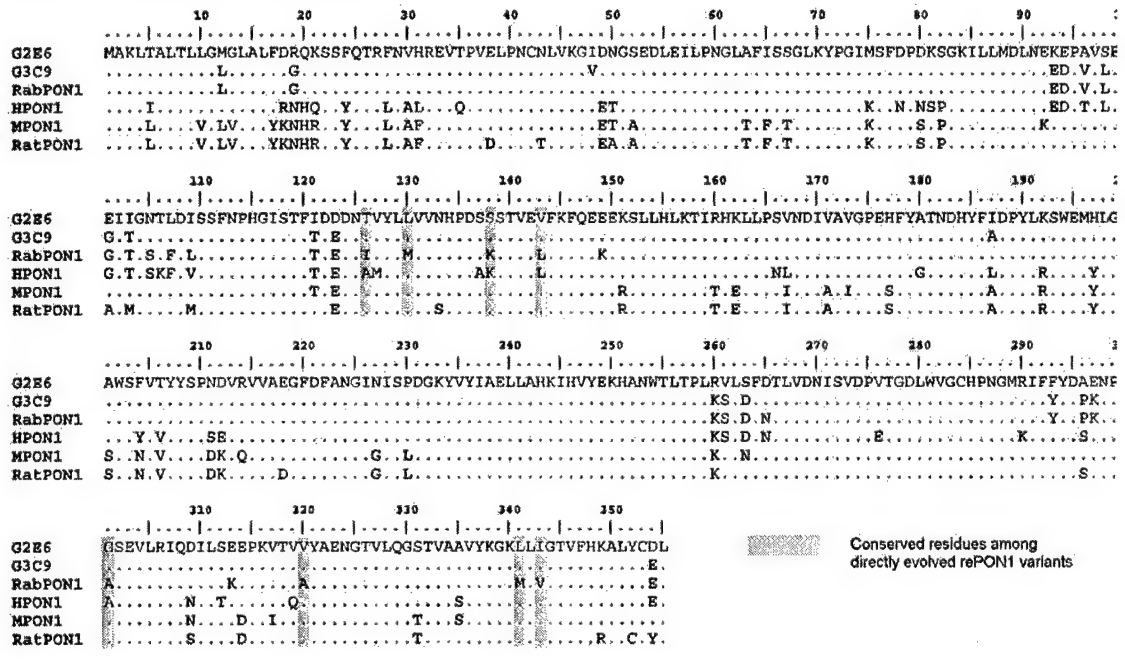

Fig 6. Multiple sequence alignment of human (H), rat, mouse (M) and rabbit (Rab) PON1, and rePON1 variants G2E6 and G3C9.

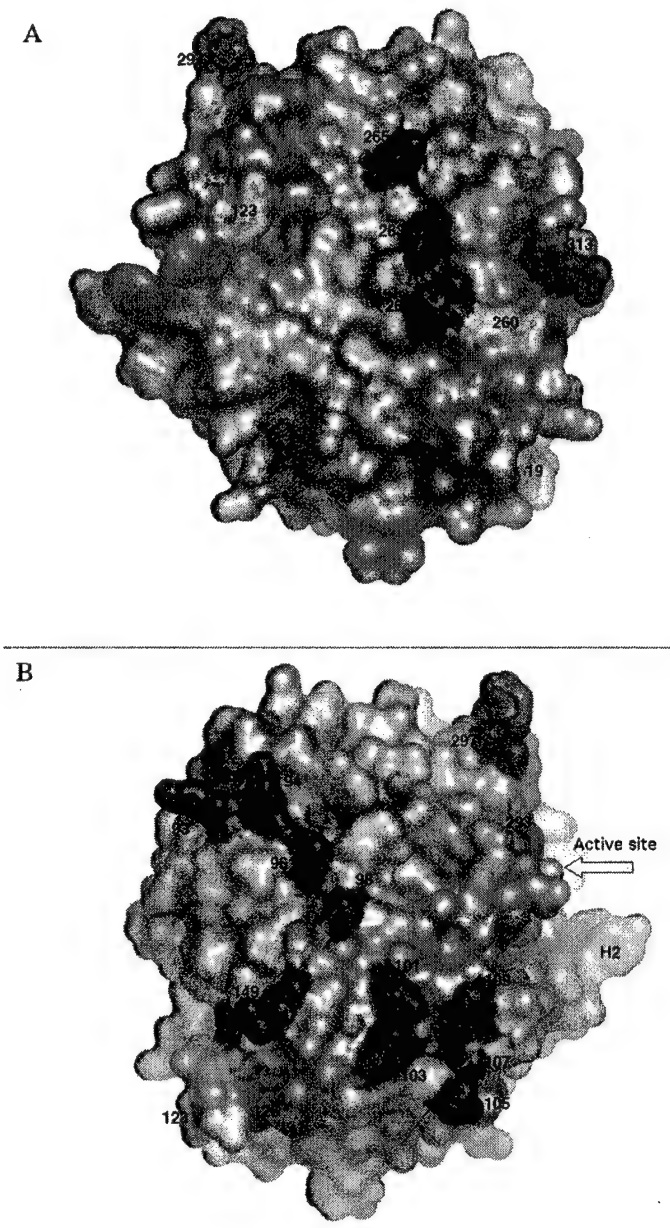

Fig 7. Two surface representations taken from the side of the β-propeller – one rotated 180° relative to the other. The amino acid variations between rePON1 variant G2E6 and wt RabPON1 are marked: In red are amino acids that originate from Human, Mouse and Rat PON1 and are conserved among all the rePON1 variants expressed in *E. coli* (Table 1, group I). In blue - amino acids that originate from Human, Mouse and Rat PON1 which are *not* conserved among soluble rePON1 variants (Table 1, group II). In green - amino acids that were mutated during the DNA shuffling process (Table 4, group III). The figure was created by PyMol (http://pymol.sourceforge.net/).

Key Research Accomplishments

- 6 new PON1 variants were generated by directed evolution:
  - 7PC – V346A
  - 4PC – L69V, S193P, V346A
  - 1HT – I291L, T332A, G339E]
  - 2AC – F292S, V346M, V30A, E249K
  - 7HY – F292V, Y293D, I109M,
  - 4HY – I74L, F292L, K84Q, I343M
- These new PON1 variants displayed a repertoire of specificities towards ester and organophosphate substrates, thus demonstrating the potential to engineer variants with beneficial scavenger activities.
- Crystals of RePON1-G2E6 (which exhibit 91% identity to wt rabbit PON1) were obtained as were as well homologous crystals of the Se-Met derivative
- X-ray data sets were collected to for the native crystals to 2.2Å and for the Se-Met derivative to 2.6Å resolution.
- The X-ray data sets were used to determine, for the first time, the 3D crystal structure of paraoxonase.
- The 3D structure permitted identification of the active site and led to a proposed catalytic mechanism of paraoxonase

Reportable Outcomes

Manuscripts:

1. Aharoni, A., Gaidukov, L., Yagur, S., Toker, L., Silman, I. & Tawfik, D.S. (2004). "Directed evolution of mammalian paraoxonases PON1 and PON3 for bacterial expression and catalytic specialization" *Proc. Natl. Acad. Sci. USA* **101**, 482-487.
2. Harel, M., Aharoni, A., Gaidukov, L., Brumshtein, B., Khersonsky, O., Meged, R., Dvir, H., Ravelli, R.B., McCarthy, A., Toker, L., Silman, I., Sussman, J.L. & Tawfik, D.S. (2004). "Structure and evolution of the serum paraoxonase family of detoxifying and anti-atherosclerotic enzymes" *Nat. Struct. Mol. Biol.* **11**, 412-419.
3. Harel, M., Aharoni, A., Gaidukov, L., Brumshtein, B., Khersonsky, O., Meged, R., Dvir, H., Ravelli, R.B., McCarthy, A., Toker, L., Silman, I., Sussman, J.L. & Tawfik, D.S. (2004). "Corrigendum: Structure and evolution of the serum paraoxonase family of detoxifying and anti-atherosclerotic enzymes" *Nat. Struct. Mol. Biol.* **11**, 1253.

Abstracts:

1. Aharoni, A. (2004) "Directed Evolution of Paraoxonases PON1 and PON3 for Bacterial Expression and Catalytic Specialization" First International Conference on "Paraoxonases - Basic and Clinical Directions of Current Research" 22-24 April 2004, Michigan Union, University of Michigan, Ann Arbor, USA.
2. Sussman, J.L. (2004) "The 3D-Structure, Mechanism and Evolution of Serum Paraoxonases" 22-24 April 2004, Michigan Union, University of Michigan, Ann Arbor, USA.
3. Sussman, J.L, Aharoni, A., Harel, M., Gaydukov, L., Brumshtein, B., Meged, R., Khersonsky, O., Toker, L., Silman, I. & Tawfik, D.S. (2004) "3D Structure of Mammalian Paraoxonase at 2.2Å Resolution" 2004 Medical Defense Bioscience Review, 16-21 May 2004, Hunt Valley, MD, USA.
4. Sussman, J.L., Silman, I., Harel, M., Aharoni, A., Gaidukov, L, Brumshtein, B. Khersonsky, O., Toker, L., & Tawfik, D.S. (2004) "The 3D-Structure, Mechanism and Evolution of Serum Paraoxonases" DECON 2004, 16-20 May 2004, Palm Harbor, FL, USA

5. Sussman, J.L. (2004) "3D-Structure, Mechanism and Evolution of Serum Paraoxonases – a Family of Detoxifying and Anti-Atherosclerotic Enzymes" Life Science Seminar, 15-June-2004, Brookhaven National Laboratory, Upton, NY, USA

Conclusions

Directed molecular evolution, which involved shuffling of the PON1 genes of four mammalian species, was used to produce soluble and catalytically active paraoxonase in *E. coli* in milligram quantities. A number of different mutants were produced which differed in their specificity towards ester and organophosphate substrates. These findings demonstrate the potential of molecular evolution to generate PON1 variants tailor made for serving as nerve agent scavengers.

One new variant was crystallized and its crystal structure subsequently determined. The 3D structure was revealed to be a 6-blade β-propeller. The active was found to be within the central cavity of the propeller and a plausible reaction mechanism was suggested.

References

1. Draganov, D.I. & La Du, B.N. Pharmacogenetics of paraoxonases: a brief review. *Naunyn Schmiedebergs Arch Pharmacol* **369**, 78-88 (2004).
2. Lusis, A.J. Atherosclerosis. *Nature* **407**, 233-241 (2000).
3. Shih, D.M., Gu, L., Xia, Y.R., Navab, M., Li, W.F., Hama, S., Castellani, L.W., Furlong, C.E., Costa, L.G., Fogelman, A.M. & Lusis, A.J. Mice lacking serum paraoxonase are susceptible to organophosphate toxicity and atherosclerosis. *Nature* **394**, 284-287 (1998).
4. Mackness, M.I., Arrol, S. & Durrington, P.N. Paraoxonase prevents accumulation of lipoperoxides in low-density lipoprotein. *FEBS Lett* **286**, 152-154 (1991).
5. Reddy, S.T., Wadleigh, D.J., Grijalva, V., Ng, C., Hama, S., Gangopadhyay, A., Shih, D.M., Lusis, A.J., Navab, M. & Fogelman, A.M. Human paraoxonase-3 is an HDL-associated enzyme with biological activity similar to paraoxonase-1 protein but is not regulated by oxidized lipids. *Arterioscler Thromb Vasc Biol* **21**, 542-547 (2001).
6. Rodrigo, L., Mackness, B., Durrington, P.N., Hernandez, A. & Mackness, M.I. Hydrolysis of platelet-activating factor by human serum paraoxonase. *Biochem J* **354**, 1-7 (2001).
7. Ahmed, Z., Ravandi, A., Maguire, G.F., Emili, A., Draganov, D., La Du, B.N., Kuksis, A. & Connelly, P.W. Apolipoprotein A-I promotes the formation of phosphatidylcholine core aldehydes that are hydrolyzed by paraoxonase (PON-1) during high density lipoprotein oxidation with a peroxynitrite donor. *J Biol Chem* **276**, 24473-24481 (2001).
8. Jakubowski, H. Calcium-dependent human serum homocysteine thiolactone hydrolase. A protective mechanism against protein N-homocysteinylation. *J Biol Chem* **275**, 3957-3962 (2000).
9. Sorenson, R.C., Bisgaier, C.L., Aviram, M., Hsu, C., Billecke, S. & La Du, B.N. Human serum Paraoxonase/Arylesterase's retained hydrophobic N-terminal leader sequence associates with HDLs by binding phospholipids : apolipoprotein A-I stabilizes activity. *Arterioscler Thromb Vasc Biol* **19**, 2214-2225 (1999).
10. Aharoni, A., Gaidukov, L., Yagur, S., Toker, L., Silman, I. & Tawfik, D.S. Directed evolution of mammalian paraoxonases PON1 and PON3 for bacterial expression and catalytic specialization. *Proc Natl Acad Sci USA* **101**, 482-487 (2004).
11. Fokine, A., Morales, R., Contreras-Martel, C., Carpentier, P., Renault, F., Rochu, D. & Chabriere, E. Direct phasing at low resolution of a protein copurified with human paraoxonase (PON1). *Acta Crystallogr D Biol Crystallogr* **59**, 2083-2087 (2003).
12. Josse, D., Ebel, C., Stroebel, D., Fontaine, A., Borges, F., Echalier, A., Baud, D., Renault, F., Le Maire, M., Chabrieres, E. & Masson, P. Oligomeric states of the detergent-solubilized human serum paraoxonase (PON1). *J Biol Chem* **277**, 33386-33397 (2002).
13. Kuo, C.L. & La Du, B.N. Comparison of purified human and rabbit serum paraoxonases. *Drug Metab Dispos* **23**, 935-944 (1995).
14. Harel, M., Aharoni, A., Gaidukov, L., Brumshtein, B., Khersonsky, O., Meged, R., Dvir, H., Ravelli, R.B., McCarthy, A., Toker, L., Silman, I., Sussman, J.L. & Tawfik, D.S. Structure and evolution of the serum paraoxonase family of detoxifying and anti-atherosclerotic enzymes. *Nat Struct Mol Biol* **11**, 412-419 (2004).

15. Jawad, Z. & Paoli, M. Novel sequences propel familiar folds. *Structure (Camb)* **10**, 447-454 (2002).
16. Kuo, C.L. & La Du, B.N. Calcium binding by human and rabbit serum paraoxonases. Structural stability and enzymatic activity. *Drug Metab Dispos* **26**, 653-660 (1998).
17. Scharff, E.I., Koepke, J., Fritzsch, G., Lucke, C. & Ruterjans, H. Crystal structure of diisopropylfluorophosphatase from Loligo vulgaris. *Structure (Camb)* **9**, 493-502 (2001).
18. Josse, D., Xie, W., Renault, F., Rochu, D., Schopfer, L.M., Masson, P. & Lockridge, O. Identification of residues essential for human paraoxonase (PON1) arylesterase/organophosphatase activities. *Biochemistry* **38**, 2816-2825 (1999).
19. Josse, D., Lockridge, O., Xie, W., Bartels, C.F., Schopfer, L.M. & Masson, P. The active site of human paraoxonase (PON1). *J Appl Toxicol* **21 Suppl 1**, S7-S11 (2001).
20. Josse, D., Xie, W., Masson, P., Schopfer, L.M. & Lockridge, O. Tryptophan residue(s) as major components of the human serum paraoxonase active site. *Chem Biol Interactions* **119-120**, 79-84 (1999).
21. Sekar, K., Yu, B.Z., Rogers, J., Lutton, J., Liu, X., Chen, X., Tsai, M.D., Jain, M.K. & Sundaralingam, M. Phospholipase A2 engineering. Structural and functional roles of the highly conserved active site residue aspartate-99. *Biochemistry* **36**, 3104-3114 (1997).
22. Yeung, D.T., Josse, D., Nicholson, J.D., Khanal, A., McAndrew, C.W., Bahnson, B.J., Lenz, D.E. & Cerasoli, D.M. Structure/function analyses of human serum paraoxonase (HuPON1) mutants designed from a DFPase-like homology model. *Biochim Biophys Acta* **1702**, 67-77 (2004).
23. Harel, M., Aharoni, A., Gaidukov, L., Brumshtein, B., Khersonsky, O., Meged, R., Dvir, H., Ravelli, R.B., McCarthy, A., Toker, L., Silman, I., Sussman, J.L. & Tawfik, D.S. Corrigendum: Structure and evolution of the serum paraoxonase family of detoxifying and anti-atherosclerotic enzymes. *Nat Struct Mol Biol* **11**, 1253 (2004).
24. Aviram, M., Billecke, S., Sorenson, R., Bisgaier, C., Newton, R., Rosenblat, M., Erogul, J., Hsu, C., Dunlop, C. & La Du, B. Paraoxonase active site required for protection against LDL oxidation involves its free sulfhydryl group and is different from that required for its arylesterase/paraoxonase activities: selective action of human paraoxonase allozymes Q and R. *Arterioscler Thromb Vasc Biol* **18**, 1617-1624 (1998).
25. Borhani, D.W., Rogers, D.P., Engler, J.A. & Brouillette, C.G. Crystal structure of truncated human apolipoprotein A-I suggests a lipid-bound conformation. *Proc Natl Acad Sci USA* **94**, 12291-12296 (1997).
26. Segrest, J.P., Harvey, S.C. & Zannis, V. Detailed molecular model of apolipoprotein A-I on the surface of high-density lipoproteins and its functional implications. *Trends Cardiovasc Med* **10**, 246-252 (2000).
27. Killian, J.A. & von Heijne, G. How proteins adapt to a membrane-water interface. *TIBS* **25**, 429-434 (2000).
28. Bencharit, S., Morton, C.L., Xue, Y., Potter, P.M. & Redinbo, M.R. Structural basis of heroin and cocaine metabolism by a promiscuous human drug-processing enzyme. *Nat Struct Biol* **10**, 349-356 (2003).

29. Millard, C.B., Lockridge, O. & Broomfield, C.A. Organophosphorus acid anhydride hydrolase activity in human butyrylcholinesterase: synergy results in a somanase. *Biochemistry* **37**, 237-247 (1998).
30. Greenblatt, H.M., Dvir, H., Silman, I. & Sussman, J.L. Acetylcholinesterase: a multifaceted target for structure-based drug design of anticholinesterase agents for the treatment of Alzheimer's disease. *J Mol Neurosci* **20**, 369-384 (2003).
31. Leviev, I., Deakin, S. & James, R.W. Decreased stability of the M54 isoform of paraoxonase as a contributory factor to variations in human serum paraoxonase concentrations. *J Lipid Res* **42**, 528-535 (2001).
32. Chayen, N.E., Stewart, P.D.S., Maeder, D.L. & Blow, D.M. An Automated System for Micro-Batch Protein Crystallization and Screening. *J Appl Cryst* **23**, 297-302 (1990).
33. Kabsch, W. Automatic processing of rotation diffraction data from crystals of initially unknown symmetry and cell constants. *J Appl Cryst* **26**, 795-800 (1993).
34. Storoni, L.C., McCoy, A.J. & Read, R.J. Likelihood-enhanced fast rotation functions. *Acta Crystallogr D Biol Crystallogr* **60**, 432-438 (2004).
35. Uson, I. & Sheldrick, G.M. Advances in direct methods for protein crystallography. *Curr Opin Struct Biol* **9**, 643-648 (1999).
36. de La Fortelle, E. & Bricogne, G. "MaximumLikelihood Heavy-Atom Parameter Refinement in the MIR and MAD Methods". in *Methods in Enzymology*, Vol. 276 (eds. Carter, C.W. & Sweet, R.M.) 472-494 (Academic Press, 1996).
37. Abrahams, J.P. & Leslie, A.G. Methods used in the structure determination of bovine mitochondrial F1 ATPase. *Acta Crystallogr D Biol Crystallogr* **52**, 30-42 (1996).
38. Perrakis, A., Morris, R. & Lamzin, V.S. Automated protein model building combined with iterative structure refinement. *Nat Struct Biol* **6**, 458-463 (1999).
39. Jones, T.A., Zou, J.-Y., Cowan, S.W. & Kjeldgaard, M. Improved methods for building protein models in electron density maps and the location of errors in these models. *Acta Cryst* **A47**, 110-119 (1991).
40. Murshudov, G.N., Vagin, A.A., Lebedev, A., Wilson, K.S. & Dodson, E.J. Efficient anisotropic refinement of macromolecular structures using FFT. *Acta Crystallogr D Biol Crystallogr* **55 (Pt 1)**, 247-255 (1999).
41. Lee, B.K. & Richards, F.M. The Interpretation of Protein Structures Estimation of Static Accessibility. *J Mol Biol* **55**, 379-400 (1971).

Appendices

none